Frontiers of Information Technology & Electronic Engineering
www.jzus.zju.edu.cn; engineering.cae.cn; www.springerlink.com
ISSN 2095-9184 (print); ISSN 2095-9230 (online)
E-mail: jzus@zju.edu.cn

Review:

Recent advances in multisensor multitarget tracking using random finite set*

Kai DA[†1], Tiancheng LI[†‡2], Yongfeng ZHU[†1], Hongqi FAN[†1], Qiang FU[1]

[1]*The National Key Laboratory of Science and Technology on ATR, National University of Defense Technology, Changsha 410073, China*

[2]*MOE Key Laboratory of Information Fusion Technology, School of Automation, Northwestern Polytechnical University, Xi'an 710072, China*

[†]E-mail: dktm131@163.com; t.c.li@nwpu.edu.cn; zoyofo@163.com; fanhongqi@nudt.edu.cn

Received June 1, 2020; Revision accepted July 17, 2020; Crosschecked Sept. 11, 2020

Abstract: In this study, we provide an overview of recent advances in multisensor multitarget tracking based on the random finite set (RFS) approach. The fusion that plays a fundamental role in multisensor filtering is classified into data-level multitarget measurement fusion and estimate-level multitarget density fusion, which share and fuse local measurements and posterior densities between sensors, respectively. Important properties of each fusion rule including the optimality and sub-optimality are presented. In particular, two robust multitarget density-averaging approaches, arithmetic- and geometric-average fusion, are addressed in detail for various RFSs. Relevant research topics and remaining challenges are highlighted.

Key words: Multitarget tracking; Multisensor fusion; Average fusion; Random finite set; Optimal fusion
https://doi.org/10.1631/FITEE.2000266 **CLC number:** TP273.5

1 Introduction

Multitarget tracking (MTT) refers to joint estimation of the number and states of targets from noisy observations in the presence of random target birth/death and missing/false data. Benchmark MTT algorithms include the joint (integrated) probabilistic data association filter (Musicki and Evans, 2004; Bar-Shalom et al., 2011) and (probabilistic) multiple-hypothesis tracker (Blackman et al., 1999; Willett et al., 2002). Compared with these classic theories and algorithms, the random finite set (RFS) provides a new unified and fully probabilistic approach to MTT and information fusion (Mahler, 2007b, 2014) and has rapidly developed along diverse pathways over the last two decades (Streit et al., 2015; Vo BN et al., 2015; Williams, 2015; Meyer et al., 2018). One theme that has attracted much attention is tangled with wireless sensor networks (WSNs), where MTT is implemented by multiple/massive sensors in parallel. A simple MTT scene using two sensors is illustrated in Fig. 1. Simply put, fusion between two sensors will increase the information of each to achieve better estimation.

The wide distribution of sensor nets in civilian life and in many important industrial realms has the advantages of improving estimation accuracy, extending tracking coverage, and enhancing the viability/scalability of sensors. In particular, the distributed network is more robust and less prone to single-point failures than the centralized

‡ Corresponding author

* Project supported by the Key Laboratory Foundation of National Defence Technology, China (No. 61424010306), the Joint Fund of Equipment Development and Aerospace Science and Technology, China (No. 6141B0624050101), and the National Natural Science Foundation of China (Nos. 61901489 and 62071389)

ORCID: Kai DA, https://orcid.org/0000-0002-6645-2881; Tiancheng LI, https://orcid.org/0000-0002-0499-5135

network. This has in turn significantly promoted the development of RFS-based tracking approaches. In this review, we focus on multisensory RFS-based MTT. Our work complements some recent monographs/overviews on the relevant topics, such as Liggins et al. (2008), Chen X et al. (2014), Farina et al. (2017), Chong et al. (2018), He et al. (2020), and Javadi and Farina (2020).

Existing multisensor MTT approaches can be classified into two major groups depending on the type of information shared between sensors: these are data-level multitarget measurement fusion and estimate-level multitarget density fusion, as shown in Fig. 2. Briefly speaking, the majority of the former group is dedicated to computing the joint likelihood of all measurements of all sensors, approaching the optimal multisensor Bayes posterior. Then, raw measurements must be transmitted between sensors,

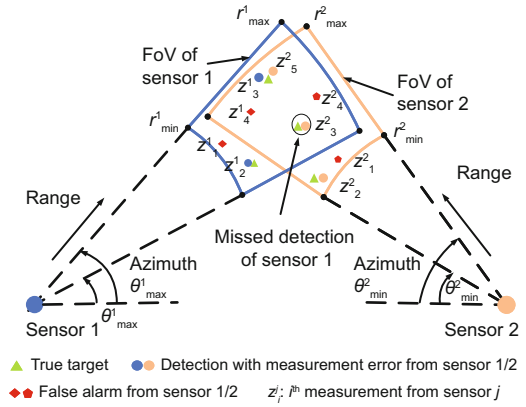

Fig. 1 A multitarget tracking scene using two active radars

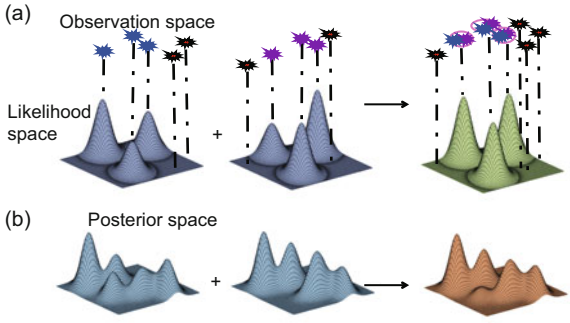

Fig. 2 Two major groups of the existing multisensor multitarget tracking approaches: (a) data-level fusion: raw measurements from different sensors are used to calculate the multisensor joint likelihood at each sensor; (b) estimate-level fusion: each sensor uses its own measurements for the filtering calculation, the results of which (called "posteriors") are fused across sensors

which might be heterogeneous and asynchronous and the joint-likelihood function may be computationally intractable. By contrast, multisensor-density fusion fuses the posterior densities yielded by the local sensors, which in tandem with the popular-consensus approach, leads to a robust and fault-tolerant approach to multisensor MTT. This fusion is, however, typically suboptimal due to the omitted cross-correlation between densities. All these issues are to be detailed in this study.

Abbreviations and symbols are summarized in Tables 1 and 2, respectively.

Table 1 Abbreviations

Abbreviation	Full name
AA	Arithmetic average
BC	Bernoulli component
CPHD	Cardinalized PHD
CBMeMber	Cardinality-balanced MeMber
FoV	Field of view
GA	Geometric average
GM	Gaussian mixture
GLMB	Generalized labeled multi-Bernoulli
IC	Iterated-corrector
IIDC	Identical, independently distributed cluster
KLD	Kullback-Leibler divergence
LMB	Labeled multi-Bernoulli
MB	Multi-Bernoulli
MBM	Multi-Bernoulli mixture
MeMber	Multitarget multi-Bernoulli
MPD	Multitarget probability distribution
MTT	Multitarget tracking
PCAM	Parallel combination approximate multisensor
PMBM	Poisson multi-Bernoulli mixture
PHD	Probability hypothesis density
RFS	Random finite set
WSN	Wireless sensor network

2 Random finite set

An RFS X in space $\mathbb{X}$ is a random variable taken from $\mathcal{F}(\mathbb{X})$, which can naturally characterize the false alarms, missed detections, and births and deaths of targets. A real-valued function $f(X)$ is a multitarget density function of X if its unit is $u^{-|X|}$, where u is the unit of $x \in X$. If $\int f(X)\delta X = 1$ is satisfied, then $f(X)$ is also called the multitarget probability density function (MPD), where the set integral is defined with respect to any region S by

Table 2 Mathematical symbols

Symbol	Meaning
X	Multitarget state
$\|X\|$	Number of elements in X
$\mathbb{X}$	State space
$\mathcal{F}(\mathbb{X})$	Collection of finite subsets of $\mathbb{X}$
L	Label set
$\mathbb{L}$	Label space
$\mathcal{L}(X)$	The set of labels of X
Z_k^i	Measurements of the i^{th} sensor at time k
m^i	Number of measurements of sensor i
$f(X)$	Multitarget density function
$D(x)$	PHD function
$p(n)$	Cardinality distribution
$s(x)$	Spatial single-target density
λ	The expected number of targets
$p_{\mathrm{S}}(\cdot)$	Target survival probability
$p_{\mathrm{D}}(\cdot)$	Detection probability
$\Phi_{k\|k-1}(\cdot\|\cdot)$	State transition function
$g_k(\cdot\|\cdot)$	Target-likelihood function at time k
$\delta(x)$	Dirac delta function
$1_X(x)$	Equals 1 if $x \subseteq X$; otherwise, equals 0
$\langle f, g\rangle$	$\int f(x)g(x)\mathrm{d}x$
h^X	Multitarget exponential $\prod_{x\in X} h(x)$, $h^{\varnothing} = 0$
$\mathcal{N}^j$	The set of neighbors of sensor j, including j
$\uplus$	Disjoint union operation
r_i	Existence probability of BC i
$\Delta(X)$	The distinct-label indicator (equals 1 if $\|X\| = \|\mathcal{L}(X)\|$; otherwise, equals 0)
Ξ	Track-to-measurement association history

$$\int_S f(X)\delta X = f(\varnothing) + \sum_{n=1}^{\infty} \frac{1}{n!} \int_{S^n} f(\{x_1, x_2, \ldots, x_n\})\mathrm{d}x_1\mathrm{d}x_2 \ldots \mathrm{d}x_n.$$

Note that another fundamental descriptor for characterizing RFS is the void probability (Beard et al., 2017), i.e., the probability that the corresponding region containing no points of the point process.

The first order of X, namely the probability hypothesis density (PHD), is defined as

$$D(x) = \int f(\{x\} \cup X)\, \delta X. \tag{1}$$

The integral of PHD $\int_S D(x)\mathrm{d}x$ in a region S denotes the expected number of targets in that region. The cardinality distribution is defined by

$$p(n) = \int_{|Y|=n} f(X)\delta X, \tag{2}$$

where $p(n)$ means the probability that there are n elements in X.

2.1 Multitarget motion/observation model

Given the target states at time $k-1$ denoted by an RFS $X_{k-1} = \{x'_1, x'_2, \ldots, x'_{n'}\}$, each target $x' \in X_{k-1}$ may persist with a probability $p_{\mathrm{S}}(x)$ or disappear with a probability $1 - p_{\mathrm{S}}(x)$ at time k. That is,

$$T(x') = \begin{cases} \varnothing, & \text{if disappears (prob. } 1 - p_{\mathrm{S}}(x)), \\ \{x\}, & \text{if persists (prob. } p_{\mathrm{S}}(x)), \end{cases}$$

where $\{x\}$ is the state with distribution $\Phi_{k|k-1}(x|x')$. Then, the RFS motion model is given by

$$X_{k|k-1} = T(x'_1) \cup T(x'_2) \cup \ldots \cup T(x'_{n'}) \cup B_k \cup \Gamma_k, \tag{3}$$

where B_k is the set of newly appearing targets and Γ_k is the set of spawned targets at time k.

Consider the standard measurement model; i.e., each target generates at most a single measurement, and any measurement is generated by at most a single target. Given the target RFS $X_k = \{x_1, x_2, \ldots, x_n\}$, each target $x \in X_k$ generates a measurement with probability $p_{\mathrm{D}}(x)$. That is,

$$\Upsilon(x_i) = \begin{cases} \varnothing, & \text{if undetected (prob. } 1 - p_{\mathrm{D}}(x)), \\ \{z_i\}, & \text{if detected (prob. } p_{\mathrm{D}}(x)), \end{cases}$$

where $\{z_i\}$ is the measurement with distribution $g_k(z|x_i)$. The RFS-based measurement model is given by

$$Z_k = \Upsilon(x_1) \cup \Upsilon(x_2) \cup \ldots \cup \Upsilon(x_n) \cup C_k, \tag{4}$$

where C_k is the set of measurements generated by clutter.

Usually, the above dynamic and measurement models are described by the Markov multitarget-transition density, $\Phi_{k|k-1}(X|X')$, and the multitarget-likelihood function, $g_k(Z_k|X_k)$, respectively.

2.2 RFS-based filters

On the basis of the models in Section 2.1, the theoretically optimal multitarget Bayesian filter is given by the following prediction and correction steps:

$$f_{k|k-1}(X|Z_{1:k-1}) = \int \Phi_{k|k-1}(X|X') f_{k-1}(X'|Z_{1:k-1})\delta X', \tag{5}$$

$$f_k(X|Z_{1:k}) = \frac{g_k(Z_k|X)f_{k|k-1}(X|Z_{1:k-1})}{\int g_k(Z_k|X)f_{k|k-1}(X|Z_{1:k-1})\delta X}. \tag{6}$$

The multitarget state-extraction step, during which an expected a posteriori estimator or a maximum a posteriori estimator may be used, acts upon the updated posterior density to extract the target states at the end of the iteration. The optimal multitarget Bayesian filter involving multitarget integrals is computationally intractable in practice; consequently, a set of principled approximate filters have been proposed under different RFS assumptions (Mahler, 2007b).

2.2.1 IIDC/Poisson RFS

An IIDC RFS X is one in which the elements have an identical and independent distribution $s(x)$, and in which the cardinality distribution of X is $p(n)$. The MPD and PHD associated with the IIDC RFS X are given by

$$f^{\mathrm{iidc}}(X) = n!p(n)\prod_{x\in X} s(x), \tag{7}$$

$$D^{\mathrm{iidc}}(x) = \sum_{n=0}^{\infty} np(n)s(x). \tag{8}$$

Poisson RFS is a special IIDC RFS for which the cardinality distribution $p(n)$ is Poisson with a mean of λ. The MPD and PHD associated with the Poisson RFS X are given by

$$f^{\mathrm{p}}(X) = \mathrm{e}^{-\lambda}\prod_{x\in X}\lambda s(x), \quad D^{\mathrm{p}}(x) = \lambda s(x). \tag{9}$$

The PHD filter (Mahler, 2003; Vo BN et al., 2005; Vo BN and Ma, 2006) assumes that the predicted MPD is Poisson and recursively propagates the PHD of the Poisson RFS. The CPHD filter (Mahler, 2007a; Vo BT et al., 2007), by contrast, assumes that both predicted and updated MPDs are IIDCs and recursively propagates the PHD and the cardinality distribution, resulting in a better estimate of the number of targets but with higher complexity.

2.2.2 (Multi-)Bernoulli RFS

A Bernoulli RFS X either contains a single target with a probability of r or is empty with a probability of $1-r$. The MPD of the Bernoulli RFS is given by

$$f^{\mathrm{b}}(X) = \begin{cases} 1-r, & X = \varnothing, \\ rs(x), & X = \{x\}, \\ 0, & |X| \geq 2. \end{cases} \tag{10}$$

A multi-Bernoulli (MB) RFS X is the union of n independent Bernoulli RFSs. The MPD and PHD of an MB RFS X have forms given as follows:

$$f^{\mathrm{mb}}(X) = \sum_{X_1\uplus X_2\uplus\ldots\uplus X_n}\prod_{i=1}^{n} f_i^{\mathrm{b}}(X_i), \tag{11}$$

$$D^{\mathrm{mb}}(x) = \sum_{i=1}^{n} r_i s_i(x). \tag{12}$$

The Bernoulli filter (Vo BT, 2008; Ristic et al., 2013b) is Bayesian optimal for detecting and tracking at most one target in an arbitrary clutter background and detection profile. It recursively propagates the Bernoulli parameters of the spatial single-target density and existence probability. Similarly, the MeMber filter (Mahler, 2007b) recursively propagates MB parameters rather than the MB distribution. The original MeMBer filter has an upward-cardinality bias that is corrected in the CBMeMBer filter (Vo BT et al., 2009, 2013).

2.2.3 PMBM RFS

A PMBM RFS (Granström et al., 2015; Williams, 2015; García-Fernández et al., 2018) is the convolution of a Poisson RFS and an MBM RFS with an MPD as follows:

$$f^{\mathrm{pmbm}}(X) = \sum_{Y\uplus W=X} f^{\mathrm{p}}(Y)f^{\mathrm{mbm}}(W), \tag{13}$$

where $f^{p}(\cdot)$ is a Poisson density and represents all undetected targets. The MBM density $f^{\mathrm{mbm}}(\cdot)$ representing potentially detected targets is a weighted sum of MPDs of MB and has the form

$$f^{\mathrm{mbm}}(X) \propto \sum_{j\in\mathbb{J}}\sum_{X_1\uplus X_2\uplus\ldots\uplus X_n=X}\prod_{i=1}^{n} w_{j,i}f_{j,i}^{\mathrm{b}}(X_i), \tag{14}$$

where j is an index over all global hypotheses (components of the mixtures), $\mathbb{J}$ is the index set of MBs in the MBM (with each term corresponding to a global-association hypothesis).

As a conjugate prior under a standard-state-motion model with Poisson birth, the PMBM has a

closed-form Markov-Bayes recursion similar to that of the GLMB filter. It offers an attractive performance in the case of low target-detection probability (Xia et al., 2017; Smith et al., 2019).

2.2.4 Labeled RFS

On the basis of the conventional RFS, a labeled RFS $X=\{(x_1,l_1),(x_2,l_2),\dots,(x_n,l_n)\}\subseteq\mathbb{X}\times\mathbb{L}$ serves to append distinct labels $l_1,l_2,\dots,l_n\in\mathbb{L}$ to the elements in an RFS. The most known labeled RFS, namely the GLMB RFS, which can be converted into the labeled IIDC RFS or LMB RFS, is a mixture of multitarget exponentials with probability density (Vo BT and Vo, 2013)

$$f^{\mathrm{gl}}(X)=\Delta(X)\sum_{c\in\mathbb{C}}\omega^{(c)}(\mathcal{L}(X))\prod_{(x,l)\in X}s^{(c)}(x,l), \tag{15}$$

where $\mathbb{C}$ is a discrete index set. $\omega^{(c)}(L)$ is the weight of the hypothesis that $|X|=n$ targets are presented with respective labels $l_1,l_2,\dots,l_n\in L$ and respective probability distributions $s^{(c)}(x_1,l_1),s^{(c)}(x_2,l_2),\dots,s^{(c)}(x_n,l_n)$, satisfying $\sum_{L\subseteq\mathbb{L}}\sum_{c\in\mathbb{C}}\omega^{(c)}(L)=1$ and $\int s^{(c)}(x,l)\mathrm{d}x=1$.

The GLMB filter (Vo BT and Vo, 2013; Vo BN et al., 2014) supposes that the initial multitarget RFS in Eq. (5) is a GLMB, leading to an exact closed-form solution of the multitarget Bayesian recursion. In particular, unlike the unlabeled filters (e.g., the (C)PHD, MeMber, and PMBM filters) which require extra strategies for maintaining target tracks, the GLMB filter yields the MPDs of the entire trajectories of the targets, rather than just the most recent states, thereby eliminating problems like track fragmentation (Vo BN and Vo, 2019).

δ-GLMB RFS is a special GLMB RFS with $\mathbb{C}=\mathcal{F}(\mathbb{L})\times\Xi$, $w^{(c)}(L)=w^{(I,\xi)}\delta_I(L)$, and $s^{(c)}(x,l)=s^{(I,\xi)}(x,l)=s^{(\xi)}(x,l)$. The pair (I,ξ) represents the hypothesis that the set of tracks I has a history ξ of association maps. The MPD of δ-GLMB is of the form

$$f^{\mathrm{dgl}}(X)=\Delta(X)\sum_{(I,\xi)\in\mathcal{F}(\mathbb{L})\times\Xi}w^{(I,\xi)}\delta_I(\mathcal{L}(X))\left(s^{(\xi)}\right)^X. \tag{16}$$

In addition to the δ-GLMB filter, further simplifications of the δ-GLMB filter include the Mδ-GLMB and LMB filters (Reuter et al., 2014; Fantacci et al., 2015). The details are omitted here.

3 Multisensor measurement fusion

The optimal multisensor multitarget Bayesian-recursive filter is given by

$$f_{k|k-1}(X|Z_{1:k-1}^{1:s})=\int\Phi_{k|k-1}(X|X')f_{k-1}(X'|Z_{1:k-1}^{1:s})\delta X', \tag{17}$$

$$f_k(X|Z_{1:k}^{1:s})=\frac{g_k(Z_k^{1:s}|X)f_{k|k-1}(X|Z_{1:k-1}^{1:s})}{\int g_k(Z_k^{1:s}|X)f_{k|k-1}(X|Z_{1:k-1}^{1:s})\delta X}. \tag{18}$$

If the sensors observe the same targets and their measurements are conditionally independent, then

$$g(Z^1,Z^2,\dots,Z^s|X)=\prod_{i=1}^{n}g^i(Z^i|X). \tag{19}$$

Even though the above statistical independencies can be exploited for a drastic reduction of complexity, the multisensor MTT Bayes filter remains computationally intractable. In what follows, we introduce some heuristic methods followed by a theoretically satisfactory PCAM filter. In addition, by specifying the types of RFS in Eqs. (17) and (18), a variety of multisensor optimal RFS-based filters can be obtained. We note that in these approaches, the issue of measurement communication between sensors is ignored. A centralized network in which all sensors send their measurements directly to the fusion center is commonly assumed; however, when a distributed/decentralized sensor network is involved, the distributed-flooding algorithm (Li TC et al., 2017b, 2018a, 2018b) can be applied by which each sensor serves as a fusion center to access the measurements of the other linked sensors at different distances.

3.1 Two heuristic approaches

Two straightforward, heuristic measurement-fusion approaches are proposed. They have the advantage of accommodating different RFSs.

First, a widely used multisensor filter is the IC filter (Pham et al., 2007; Mahler, 2009a); it iteratively applies the single-sensor corrector for each sensor measurement set. This heuristic method has an obvious limitation in that the performance of the final result depends upon the sensors' processing order, which in turn depends upon the amount of information detected by sensors—the most informative sensor should be processed first. Thus,

typically those sensors with large detection probabilities should be processed before others (Nagappa and Clark, 2011). Additionally, in the IC MeMber/GLMB filter, the component-truncation and resampling steps, which are important for constraining the computational cost of the filter, should be applied with caution in the GM/particle implementation, given that the components/particles weighted low in one sensor may actually correspond to a target weighted high by other sensors.

Second, Li TC et al. (2018a) proposed to convert the collection of measurements of different sensors into a set of proxy and homologous measurements (typically positions), which overcomes the problems of false and missing data and unknown statistics, facilitating linear PHD updating that amounts to standard single-sensor PHD filtering with no false or missing data. This simple scheme, however, demonstrates promising performance for certain measurement models and scenarios. In fact, these pseudo-position measurements themselves may provide very high positioning accuracy (Li TC et al., 2018b) without modeling the dynamics of the targets.

3.2 PCAM filter

The PCAM filter is a principled approximation of the multisensor Bayesian filter (Mahler, 2010). At the core of this filter is the assumption that the measurements of distinct sensors are conditionally independent (Eq. (19)). The corrector of the multisensor multitarget Bayesian filter can be rewritten as a form of "Bayesian parallel combination" as

$$\begin{aligned} f_k(X|Z_{1:k}^{1:s}) &\propto g_k(Z_k^{1:s}|X) f_{k|k-1}(X) \\ &= g_k^1(Z_k^1|X) g_k^2(Z_k^2|X) \dots g_k^s(Z_k^s|X) f_{k|k-1}(X) \\ &= \prod_{i=1:s} f_k(X|Z_{1:k-1}^{\{1:s\}\backslash i}, Z_{1:k}^i) \big(f_{k|k-1}(X)\big)^{s-1}, \end{aligned} \tag{20}$$

where $f_{k|k-1}(X) = f_{k|k-1}(X|Z_{1:k-1}^{1:s})$ and $f_k(X|Z_{1:k-1}^{\{1:s\}\backslash i}, Z_{1:k}^i)$ is the MPD updated using the measurements of sensor i. Unlike the IC filter, the PCAM filter applies the correctors in parallel with the same predicted density, which does not depend on the sensor order.

Different PCAM RFS filters result from different assumptions about the prior $f_{k|k-1}(X)$, the singly-updated posteriors $f_k(X|Z_{1:k-1}^{\{1:s\}\backslash i}, Z_{1:k}^i)$, and the sensor-clutter processes (e.g., PCAM PHD/CPHD filter (Mahler, 2014)). However, Ouyang and Ji (2011) noted that the PCAM-PHD filter suffers from a scale-unbalance problem in the particle implementation, which worsens as the number of sensors increases. Overall, the problem of finding a computationally efficient implementation of the PCAM filters remains open.

3.3 Multisensor optimal RFS filters

3.3.1 Multisensor Bernoulli filter

The particle-based distributed Bayes-optimal Bernoulli filter was given by Papa et al. (2018); this filter approximates the Bayes-optimal estimates of the target-presence probability and the target state. This is enabled by an extension of the likelihood-consensus method (Hlinka et al., 2012), which reaches consensus with regard to the likelihood function $g(Z^1, Z^2, \dots, Z^s|X)$ as in Eq. (19) with respect to the Bernoulli process. However, so far it is unclear how to extend the likelihood-consensus approach to other RFS MTT filters.

3.3.2 Multisensor CPHD/PHD filter

The exact multisensor CPHD filter was derived by Nannuru et al. (2016) by assuming that the target birth, clutter, and predicted multitarget processes are all IIDC RFSs. A multisensor PHD filter is a special case of the multisensor CPHD filter in which the target birth, clutter, and predicted multitarget processes are modeled by Poisson RFSs (Mahler, 2009a, 2009b; Delande et al., 2010, 2011). The PHD function of the multisensor CPHD/PHD filter has the form

$$D_k(x) \propto \alpha_0 \prod_{i=1}^{s} \big(1 - p_D^i(x)\big) + \sum_{P\in\mathbb{P}} \alpha_p \left(\sum_{W\in P} \rho_W(x) \right), \tag{21}$$

where P is the partitioning of all measurements from all sensors $Z_k^{1:s}$, $W \in P$ is a subset that contains at most one measurement from sensor i, i.e., $|W^i| \le 1$, and $\mathbb{P}$ is the set of all such P's; see Nannuru et al. (2016) for details.

It can be seen that the exact implementation of the multisensor CPHD/PHD filter needs to explore all partitionings, P, of the measurements, which is computationally infeasible. A reasonable alternative is to consider only those subsets that make significant contributions to the predicted PHD function, e.g., a greedy-approach-based implementation

in Nannuru et al. (2016). Additionally, the update equations in the multisensor CPHD/PHD filter have similar forms to the single-sensor update for extended targets (Mahler, 2009c; Orguner et al., 2011). Therefore, the implementation of the multisensor CPHD/PHD filter can also benefit from those methods used to reduce the partitioning complexity for extended targets (Granström et al., 2010).

3.3.3 Multisensor MeMber filter

The exact multisensor MeMber filter was derived by Saucan et al. (2017) by assuming that the target-birth and predicted and posterior multitarget processes are all MBs and that the clutter process is Poisson. Unfortunately, the updated MPD $f_k(X)$ of the exact multisensor MeMber filter is not an MB, and thus cannot be used in the next iteration directly. However, the updated PHD $D_k(x)$ is given by

$$D_k(x)=\sum_{P\in\mathbb{P}}\alpha_P\sum_{j=1}^{M_{k|k-1}}\rho^j_{W_j}(x)s^{(j)}_{k|k-1}(x), \tag{22}$$

the detailed parameters of which were introduced in Saucan et al. (2017). This has a similar structure (i.e., a sum of weighted densities as in Eq. (12)) to that of an MB process, even though $f_k(X)$ is not an MB. Thus, an MB approximation $\hat{f}_k(X)$ with the same PHD as that of $f_k(X)$ is obtained by constructing a BC for each association between a predicted Bernoulli RFS and a partitioning (Saucan et al., 2017).

In fact, the MB approximation with the same PHD $D_k(x)$ is not unique; other choices could be clustering the updated density into a number of BCs, or finding a higher-order approximation than PHD. The implementation of the multisensor MeMber filter suffers from the same problem of measurement partitioning (Eq. (22)) as the multisensor CPHD/PHD filter does, and similar solutions can be found in Nannuru et al. (2016) and Saucan et al. (2017).

3.3.4 Multisensor GLMB filter

The exact multisensor (δ-)GLMB filter is also computationally intractable due to the assignment problem in each (δ-)GLMB update. Wei et al. (2016) developed a two-sensor δ-GLMB filter using ranked-assignment algorithms to truncate the weighted sums of the multitarget exponentials; Fantacci and Papi (2016) proposed an approximate multisensor sequential-update approach for the multisensor δ-GLMB filter. In each sequential step, an Mδ-GLMB density is used to define the principled approximation of the δ-GLMB, representing the true posterior in the sense of the multitarget Bayesian filter.

Vo BN et al. (2019) integrated the prediction and correction into a single step by inserting Eq. (18) into Eq. (17):

$$f_k(X)\propto g(Z_k^{1:s}|X)\int\Phi_{k|k-1}(X|X')f(X')\delta X', \tag{23}$$

which avoids discarding the significant components. They proposed an efficient implementation based on Gibbs sampling to truncate the δ-GLMB filtering density, leading to quadratic complexity in the number of hypothesized objects and linear complexity in the total number of measurements from all sensors.

More recently, the above mentioned measurement partitioning and Gibbs-sampling approaches have been used for multisensor PMB filtering design (with slight adjustment) (Si et al., 2020). Nevertheless, the measurement partitioning still suffers from an intractable combinatorial complexity.

Finally, we note a common misunderstanding of the communication cost incurred by radar data, which has been argued to be much higher than MPD or likelihood-parameter communication. In fact, density fusion requires the communication of a large number of GCs (weights, means, and covariances) or even particles (states and weights). They are actually more costly in communication than raw point measurements (Buonviri et al., 2019); see a case study in Li TC et al. (2018b). This is because each measurement generally corresponds to at least one GC, and the dimension of the state is usually higher than that of the measurement. This, however, may not hold for measurements like videos or images.

4 Multisensor suboptimal multitarget probability density function fusion

Rather than the above data-level multitarget measurement fusion that performs fusion before filtering, another strategy is to fuse the filtering results obtained by each sensor. That is, the sensors first

perform filtering calculations independently, and the filter results are communicated and fused at each filtering iteration. There are two basic types of results to be fused: point-estimates and posteriors (or their moments). In the former, the fusion may resort to a heuristic-data-association algorithm (Li TC et al., 2017a) in Section 5, and the fusion result may not be fed back to the filter (i.e., the fusion may yield better estimates but does not help improve the filter). What is more commonly used is the latter, which improves the posterior/moment through fusion. In what follows, we focus on the latter, and do not particularly distinguish PHD from MPD.

Notably, optimal posterior fusion requires either independence or prior knowledge of the cross-correlation between the fusing posteriors, yielding (Chong et al., 1990; Bailey et al., 2012)

$$f(X|Z^1,Z^2)\propto\frac{f(X|Z^1)f(X|Z^2)}{f(X|Z^1\cap Z^2)}, \tag{24}$$

where the denominator denotes the density of the common information between two sensors.

However, the common information between fusion MPDs is typically unknown, especially when a large WSN is involved, thus preventing Bayesian optimal fusion. Two cutting-edge suboptimal average (namely arithmetic and geometric average, or AA and GA) fusion approaches with a demonstrated ability to eschew double-counting the common information of fusing sources (Julier, 2008; Bailey et al., 2012) are reviewed in this section. Both of them are characterized as conservative fusion (Julier et al., 2006; Üney et al., 2019); that is,

$$f_{\mathrm{AA/GA}}(X|Z^1,Z^2)\geq\min\left\{f(X|Z^1),f(X|Z^2)\right\}.$$

Thus, the fusion does not overlook the probability mass at any point assigned by any fusion density.

The benefit of being conservative is obvious in practice, especially when there are unknown inputs and model mismatching. However, MPD average fusion is boosted by the connection with the popular-consensus algorithm in the context of distributed WSN. After the first WSN was realized in the 1990s, deployment of WSNs has been rapid, widespread, and fundamental. While its combination with the RFS approach has only recently become a focus, an upsurge in research has been aroused within the network-consensus framework.

4.1 Properties of AA/GA fusion

For the MPDs $f_i(X)$ from sensor $i\in\mathcal{N}^j$, their AA and GA fusions have the respective forms

$$f_{\mathrm{AA}}(X)=\sum_{i\in\mathcal{N}^j}w_if_i(X), \tag{25}$$

$$f_{\mathrm{GA}}(X)=\frac{\prod\limits_{i\in\mathcal{N}^j}\left(f_i(X)\right)^{w_i}}{\int\prod\limits_{i\in\mathcal{N}^j}\left(f_i(X)\right)^{w_i}\delta X}, \tag{26}$$

where w_i is the weight assigned to sensor i and $\sum_{i\in\mathcal{N}^j}w_i=1$.

Note that GA fusion is also popularly known as exponential mixture density (Üney et al., 2010, 2011) or generalized covariance intersection (Mahler, 2000, 2012). It is a generalization of the approach of covariance intersection (Uhlmann, 1996; Julier et al., 2006), which was originally developed for the fusion of Gaussian probability density functions despite the design of the fusion weights.

It was recently pointed out that both AA- and GA-fusion approaches are essentially Fréchet means (Li TC et al., 2020b) characterizing the central tendency of distributions in arbitrary metric spaces. For a metric space $(\mathbb{F},d(\cdot,\cdot))$, the discrete Fréchet p-mean of the densities $f_1(\cdot),f_2(\cdot),\dots,f_n(\cdot)\in\mathbb{F}$ with non-negative weights $w_1,w_2,\dots,w_n$ is defined by (Nielsen and Bhatia, 2013)

$$\mu^p(f)=\operatorname*{arg\,min}_{g(\cdot)\in\mathbb{F}}\sum_{i=1}^{n}w_id^p(g(\cdot),f_i(\cdot)), \tag{27}$$

where $d^p(g(\cdot),f(\cdot))$ is a given metric on the distance between $f(\cdot)$ and $g(\cdot)$ at power p. $\sum_{i=1}^{n}w_id^p(g(\cdot),f_i(\cdot))$ is called the Fréchet function. Da et al. (2020b) and Li TC et al. (2020b) proved that AA and GA fusions are Fréchet means using different Fréchet functions as follows:

$$f_{\mathrm{AA}}(X)=\operatorname*{arg\,min}_{g}\sum_{i\in\mathcal{N}^j}w_i||f_i-g||^2, \tag{28}$$

$$f_{\mathrm{GA}}(X)=\operatorname*{arg\,min}_{\substack{g:\\ \int g(X)\delta X=1}}\sum_{i\in\mathcal{N}^j}w_i||\log f_i-\log g||^2, \tag{29}$$

where $||f||^2=\int\left(f(X)\right)^2\delta X$.

Another property is that AA/GA fusion can be computed by minimizing the sum of the weighted KLDs between fusing and fused MPDs (Battistelli

et al., 2013; Da et al., 2019); that is,

$$f_{\mathrm{AA}}(X)=\arg\min_{g}\sum_{i\in\mathcal{N}^j}w_i D_{\mathrm{KL}}(f_i||g), \tag{30}$$

$$f_{\mathrm{GA}}(X)=\arg\min_{g:\ \int g(X)\delta X=1}\sum_{i\in\mathcal{N}^j}w_i D_{\mathrm{KL}}(g||f_i), \tag{31}$$

where $D_{\mathrm{KL}}(f||g)=\int f(X)\log\left(f(X)/g(X)\right)\delta X$.

The motivation behind these formulations (Eqs. (28)–(31)) is that both averaging-fusion approaches provide a best fit of the mixture of the fusing distributions (Li TC and Da, 2020). This best-fit property of both averaging-fusion rules has long been recognized (Heskes, 1998; Hurley, 2002; Abbas, 2009; Da et al., 2019; Li TC et al., 2019e), and has been elaborately emphasized using new terminologies (Gostar et al., 2017a; Gao et al., 2020b). It is, however, important to note that this best fit is suboptimal and what is fitted is a mixture of the fusing local posteriors, not the true multisensor posterior (Li TC and Da, 2020). The former can be viewed as a rule-of-the-thumb substitute for the latter. Through this substitution, the average fusion is connected with the optimal fusion.

4.2 Illustrative comparison between AA/GA fusion and naive fusion

Averaging for data fusion can be dated back to Roger Coats (1682–1716) (Gowing, 2002); however, averaging probability distributions yielded by different estimators is fundamentally different from averaging random variables, especially in the case of multitarget density fusion in the presence of clutter, missed detections, and measurement-origin uncertainty (Li TC et al., 2019e). The AA fusion of the distributions is a (weighted) mixture of those distributions, by which conservativeness and robustness are obtained at the price of a "flattened" distribution of larger variance (Mahler, 2013; Li TC et al., 2019e).

To illustrate this, we consider two single-target, Gaussian posterior densities with different means and covariances, as yielded by two unknown-correlated filters. Three typical scenarios are illustrated in Fig. 3. In each sub-figure, the two Gaussian densities to be fused are visualized as two ellipses, P_1 and P_2, which characterize the respective covariances, with the center points indicating the respective means. In addition to AA and GA fusion, the result of naive fusion (i.e., simply multiplying the posterior densities and disregarding their correlation) is also shown. The results of naive and GA fusion are Gaussian, while the result of AA fusion is a GM density comprising two weighted GCs. More general results have been provided by Li TC et al. (2019e), which show that the variance of the AA fusion of the densities is indeed larger than that of the GA fusion, and both are larger than that of naive fusion.

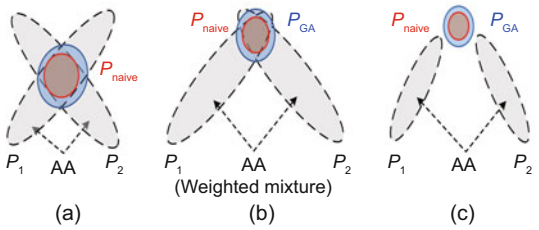

Fig. 3 Fusing two Gaussian posterior densities in three typical cases using naive, GA, and AA fusion, respectively: (a) the local densities are centered around the same position; (b) the local densities overlap only marginally; (c) the local densities are largely offset from each other

The results of naive and GA fusion are represented as red and blue ellipses, respectively, whereas the result of AA fusion is represented by the union of the two gray ellipses representing the local densities. References to color refer to the online version of this figure

However, in all the three scenarios, before we know where the true target position is relative to the effective supports of the two posterior densities to be fused, we cannot tell whether any of the three fusion schemes is better than the others, even though the covariances of the respective fusion results (as indicated by the sizes of the corresponding ellipses) differ noticeably. Even in Fig. 3a, if the target is not localized at the intersection of P_1 and P_2, then both naive and GA fusion will produce incorrect results. In Figs. 3b and 3c, at least one of the densities to be fused (P_1 or P_2) is "biased" in the sense that there is a large offset from the target position. Indeed, this is very common in most GM implementations of RFS filters, where the number of GCs is usually much larger than that of targets, such that the positions of many GCs do not conform to the state of any target.

There are other reasons why a local density (or a component of the local posterior) may be incorrect, including missed/false data and model mismatching at the respective sensor, while the other local densities may still provide an accurate representation of the target state. In the presence of measurement-origin uncertainty, it is also possible that different local densities provide accurate representations of different targets. In all of these cases, AA fusion

tends to be more robust in spite of having a larger variance, since it makes better use of the correct parts of the information provided by the local densities. This is the benefit of the "best-fit-of-mixture" performed by AA fusion (Li TC and Da, 2020), which preserves all information from all fusing posteriors. Indeed, the common merging operation and AA fusion are closely related (Li TC et al., 2017c, 2019d). What follows will compare between AA and GA fusion in more detail.

4.3 Pros & cons of AA- and GA-MPD fusion

First, the targets that are misdetected by any fusing sensor will not be contained in the GA (Li TC et al., 2017c). That is, misdetection constitutes a challenge to GA fusion. At the same time, the false alarms that occur in any fusing sensor can be entirely suppressed by GA fusion. By contrast, AA fusion preserves all target estimates from all sensors, including false alarms. Comparably speaking, GA fusion offers a better false-alarm-suppression capability, but is also more vulnerable to misdetection, whereas AA fusion can better avoid misdetection but is weaker in rejecting false alarms (Li TC et al., 2019e). Hence, GA fusion may deteriorate significantly with the increase of the number of sensors involved and with the decrease in the target-detection probability (Li TC et al., 2020b). More fusing sensors and a lower target-detection probability imply more frequent misdetection. By contrast, AA fusion performs better as the number of sensors increases: more sensors can better suppress the impact of false alarms.

Second, Üney et al. (2019) pointed out that the GA fusion of Bernoulli/Poisson/IIDC MPDs is prone to underestimating the number of targets, while the AA fusion maintains a proper cardinality unbiasedness in fusion (Li TC et al., 2019a, 2019e). Indeed, the AA of two unbiased variables remains unbiased, while their GA is in general smaller than their AA. It is relevant that GA fusion has been found to suffer from a certain delay in detecting the newborn targets (Battistelli et al., 2014; Gunay et al., 2016; Li TC et al., 2019d; Üney et al., 2019).

Third, GA fusion is more complicated than AA fusion for implementation and computation. In GM implementation, the power of GM in GA fusion is usually difficult to compute and needs to be approximated by (Julier, 2006; Battistelli et al., 2013)

$$\left(\sum N(\cdot)\right)^{w_i} \approx \sum \left(N(\cdot)\right)^{w_i}. \tag{32}$$

This approximation is valid only when Gaussian components are well separated. The particle implementation (Üney et al., 2013) of GA fusion requires a point-wise multiplication, which means that one MPD cannot be directly fused with others when the supports of particles differ from one another. Therefore, parametric-estimation approaches (Tsybakov, 2008; Sudderth et al., 2010) for converting discrete particles into a continuous approximation are often resorted to. By contrast, the GM/particle implementation of AA fusion requires only union and re-weighting operations, which can be computed much faster than GA fusion. Moreover, AA fusion is easy to perform in parallel with those components/particles. This decomposable and uncoupled feature helps develop parallel/distributed implementations.

4.4 Formulations of AA- and GA-MPD fusion

4.4.1 Fusion for unlabeled RFSs

The following theoretical results play a core role in the AA/GA fusion of various RFS filters:

Theorem 1 (AA-Bernoulli) Given the Bernoulli MPD $f_i^{\mathrm{b}}(X)$ from sensor $i \in \mathcal{N}^j$, the AA of these MPDs is still Bernoulli and has the form

$$f_w^{\mathrm{b}}(X) = \begin{cases} 1 - r_w, & X = \varnothing, \\ r_w s_w(x), & X = \{x\}, \end{cases} \tag{33}$$

where $r_w = \sum\limits_{i \in \mathcal{N}^j} w_i r_i$ and $s_w(x) = \frac{1}{r_w} \sum\limits_{i \in \mathcal{N}^j} w_i r_i s_i(x)$.

Proof The proof of this theorem can be found in Da et al. (2019) (Theorem 2) and Li TC et al. (2019b) (Lemma 1).

Theorem 2 (GA-Bernoulli) Given the Bernoulli MPD $f_i^{\mathrm{b}}(X)$ from sensor $i \in \mathcal{N}^j$, the GA of these MPDs is still Bernoulli and has the form

$$f_w^{\mathrm{b}}(X) = \begin{cases} 1 - r_w, & X = \varnothing, \\ r_w s_w(x), & X = \{x\}, \end{cases} \tag{34}$$

where $r_w = 1 - \dfrac{1}{K} \prod\limits_{i \in \mathcal{N}^j} (1 - r_i)^{w_i}$, $s_w(x) = \dfrac{1}{r_w K} \prod\limits_{i \in \mathcal{N}^j} (r_i s_i(x))^{w_i}$, and $K = \prod\limits_{i \in \mathcal{N}^j} (1 - r_i)^{w_i} + \prod\limits_{i \in \mathcal{N}^j} r_i^{w_i} \int \prod\limits_{i \in \mathcal{N}^j} (s_i(x))^{w_i} \mathrm{d}x$.

Proof The proof can be found in Clark et al. (2010) (theorem in Section 3.1).

Theorem 3 (AA-Poisson) Given the Poisson MPD $f_i^{\mathrm{p}}(X)$ from sensor $i \in \mathcal{N}^j$, the AA of these MPDs has the form $f_w(X) = \sum_{i\in\mathcal{N}^j} f_i(X)$ with PHD

$$D_w(x) = \sum_{i\in\mathcal{N}^j} w_i D_i(x). \tag{35}$$

Proof The proof can be found in Da et al. (2019) (Theorem 3) and Gao et al. (2020b) (Proposition 2). We further note that the PHD filter does not maintain or update the Poisson MPD, but only its first order moment—the PHD—over time. Therefore, one does not need to worry about the non-closure of Poisson-MPD-AA fusion. AA fusion is well motivated to be performed over the PHDs (Li TC and Hlawatsch, 2017; Li TC et al., 2019d).

Theorem 4 (GA-Poisson) Given the Poisson MPD $f_i^{\mathrm{p}}(X)$ from sensor $i \in \mathcal{N}^j$, the GA of these MPDs is still Poisson and has the form

$$f_w^{\mathrm{p}}(X) = \mathrm{e}^{-\lambda_w} \prod_{x\in X} \lambda_w s_w(x), \tag{36}$$

where $\lambda_w = \prod\limits_{i\in\mathcal{N}^j} \lambda_i^{w_i} \cdot \int \prod\limits_{i\in\mathcal{N}^j} (s_i(x))^{w_i} \mathrm{d}x$ and $s_w(x) = \dfrac{\prod\limits_{i\in\mathcal{N}^j} (s_i(x))^{w_i}}{\int \prod\limits_{i\in\mathcal{N}^j} (s_i(x))^{w_i} \mathrm{d}x}$.

Proof The proof can be found in Clark et al. (2010) (theorem in Section 3.2).

Theorem 5 (AA-IIDC) Given the IIDC MPD $f_i^{\mathrm{iidc}}(X)$ from sensor $i \in \mathcal{N}^j$, the AA fusion of the MPDs has the form $f_{\mathrm{AA}}(X) = \sum_{i\in\mathcal{N}^j} f_i(X)$ with PHD $D_{\mathrm{AA}}(x) = \sum_{i\in\mathcal{N}^j} w_i D_i(x)$ and cardinality distribution $p_{\mathrm{AA}}(n) = \sum_{i\in\mathcal{N}^j} w_i p_i(n)$, which is unfortunately no longer an IIDC MPD (i.e., it does not have closure) and cannot be used in the next iteration directly. An IIDC approximation that has the same PHD and cardinality distribution as $f_{\mathrm{AA}}(X)$ is given by

$$f_w^{\mathrm{iidc}}(X) = n! p_{\mathrm{AA}}(n) \prod_{x\in X} s_{\mathrm{AA}}(x), \tag{37}$$

where $s_{\mathrm{AA}}(x) = \dfrac{D_{\mathrm{AA}}(x)}{\sum_n n p_{\mathrm{AA}}(n)}$.

Proof The proof can be found in Da et al. (2019) (Theorem 4) and Gao et al. (2020b) (Proposition 1). It has been further proved that $f_w^{\mathrm{iidc}}(X)$ is close to $f_{\mathrm{AA}}(x)$ in the sense of minimal $D_{\mathrm{KL}}(f_{\mathrm{AA}}(X)|f_w^{\mathrm{iidc}}(X))$ (Gao et al., 2020b). We further note that the linear fusion of CPHD was first implemented in Yu et al. (2016), which, however, simply used $D_{\mathrm{AA}}(x)$ and $p_{\mathrm{AA}}(n)$ to replace the original PHD and cardinality distributions, overlooking the non-closure problem of IIDC-AA fusion.

Theorem 6 (GA-IIDC) Given the IIDC MPD $f_i^{\mathrm{iidc}}(X)$ from sensor $i \in \mathcal{N}^j$, the GA of these MPDs remains IIDC and has the form

$$f_w^{\mathrm{iidc}}(X) = n! p_w(n) \prod_{x\in X} s_w(x), \tag{38}$$

where $p_w(n) = \dfrac{\prod\limits_{i\in\mathcal{N}^j} (p_i(n))^{w_i} C^n}{\sum\limits_{m=0}^{\infty} \prod\limits_{i\in\mathcal{N}^j} (p_i(m))^{w_i} C^m}$, $s_w(x) = \frac{1}{C} \prod\limits_{i\in\mathcal{N}^j} (s_i(x))^{w_i}$, and $C = \int \prod\limits_{i\in\mathcal{N}^j} (s_i(x))^{w_i} \mathrm{d}x$.

Proof The proof can be found in Clark et al. (2010) (theorem in Section 3.2).

Theorem 7 (AA-MBM) Given the MBM MPD $f_i^{\mathrm{iidc}}(X)$ from sensor $i \in \mathcal{N}^j$, the AA of these MBMs remains an MBM.

Proof The proof can be found in Li TC and Da (2020) (Lemma 1).

The closure properties (closure property implies that the fused MPD still belongs to the same family of fusing MPDs) of GA and AA fusion for various MPDs are summarized in Table 3. However, it remains unclear whether GLMB-AA fusion admits closure. Furthermore, in view of the implementation based on GM or particles, the closure of AA and GA fusion is given in Table 4. The closure of particle-GA fusion depends upon whether the fusing distribution is represented by particles of the same state (and different weights). If so, then GA fusion preserves the same particle states with the GA-fused weights. If, however, the particle states and weights are both different, which is more common, then GA fusion must be approximated and no exact closure is

Table 3 Closure property of GA and AA fusion for different MPDs

	Bernoulli	Poisson	IIDC	MB	GLMB	MBM
AA	Yes	No	No	No	Unknown	Yes
GA	Yes	Yes	Yes	No	No	No

Table 4 Closure property of GA and AA fusion in different implementations

	GM	Particles
AA	Yes	Yes
GA	No	Depends

Particles: delta Dirac mixture

guaranteed.

The non-closure of the AA/GA fusion of MB MPDs can be addressed in two ways (Da et al., 2019). The first is fusing after association, i.e., the BCs in one MB are associated with those in the others, enabling the closure fusion of Bernoulli processes. This is referred to as the target-wise fusion rule (Li TC et al., 2020b), where two types of BC-association methods are presented based on either clustering or two-dimensional assignment. The second solution is to find a reasonable MB approximation to the AA/GA of MBs (e.g., with minor KLD). For example, Wang et al. (2017) developed a two-step-approximation method to realize GA fusion of MBs. They first approximated the GAs of two MBs to an unlabeled version of the δ-GLMB distribution, which was then approximated to a new MB that matches the PHD of the former.

4.4.2 Fusion for labeled RFSs

The fusion of labeled RFSs is more challenging due to the discrete labels. Under the ideal assumption that the labels of all fused sensors are unrealistically matched, the Mδ-GLMB and LMB MPDs are closed under GA fusion (Fantacci et al., 2018), while only the δ-GLMB MPDs are closed under AA fusion (Gao et al., 2019a). However, they suffer from a severe performance degradation when perfect label consistencies are violated (Wang et al., 2015; Li SQ et al., 2017, 2019). It is unrealistic to have perfect matching between labels from distinct sensors in practice, considering the different geographical coverage and independent birth/clutter/noise processes. In this case, one possible solution is fusing after association (Gao et al., 2019a; Li SQ et al., 2019). Another method (Jiang et al., 2016; Li SQ et al., 2017) is to marginalize the labels of each MPD to form unlabeled ones. Then, the fusion procedure is the same as their unlabeled counterparts, followed by a label-reconstruction step.

Existing labeled RFS-fusion methods essentially fuse only the target-state posterior but not the labels, which serve as no more than an indicator in the fusion. Hence, the target state posteriors but not the labels at local sensors are fused. Properly fusing labels remains an open question, which is also an important part of labeled-filter estimation. This is mainly due to the fact that the labels are estimates containing historical information and any fusion/revision of them will involve changing the historical trajectory like a smoother usually does. To illustrate this, a general example is shown in Fig. 4: the trajectories in different sensors conflict at time $k = 5$. At sensor 1, the labels/trajectories (Fig. 4a) formed by state-only fusion methods do not conform to those of the other sensors and must be revised (or else the others' labels need to be revised). Unfortunately, this is nontrivial as there are various ways to do so (Figs. 4b–4d). More importantly, this resembles smoothing and may not satisfy the real-time filtering need. Mainstream multisensor RFS filters are summarized in Table 5.

5 Remaining challenges and beyond

5.1 Fusing weight and communication mode

The performance-versus-complexity tradeoff is particularly acute in sensor networks, since collaboration between sensors comes at the cost of exchanging information between them (Li D et al., 2002). Various strategies have been employed to seek the best fusion performance while reducing the cost in both communication and fusion computation.

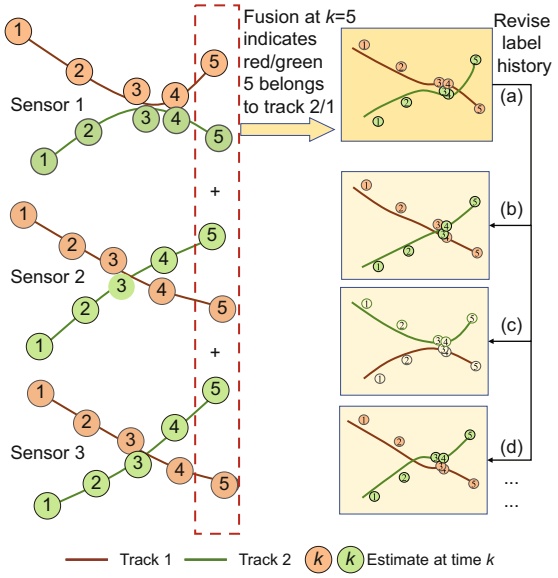

Fig. 4 Trajectories in different sensors conflict at time $k = 5$

Fusion of labels involves revising the histories/trajectories, which may lead to various results. Either way, is it still real-time fusion/filtering? References to color refer to the online version of this figure

Table 5 Mainstream multisensor RFS filters

Fusion	Heuristic	Principle approximation	
		Bayesian parallel combination	Multisensor optimal RFS-based filters
Multisensor measurement fusion	IC multisensor filter (Mahler, 2009a) Measurement clustering (Li TC et al., 2018a, 2018b)	PCAM filter (Mahler, 2010; Ouyang and Ji, 2011)	Multisensor Bernoulli filter (Hlinka et al., 2012; Papa et al., 2018) Multisensor PHD filter (Mahler, 2009a, 2009b; Delande et al., 2010, 2011) Multisensor CPHD filter (Nannuru et al., 2016) Multisensor MeMber filter (Saucan et al., 2017) Multisensor GLMB filter (Fantacci and Papi, 2016; Wei et al., 2016; Vo BN et al., 2019)
		AA (best fit of mixture)	GA (GCI/EMD)
Multisensor MPD/moments fusion	Track-to-track fusion based PHD filter without feedback to filter (Li TC et al., 2017a)	AA-Bernoulli (Da et al., 2019; Li TC et al., 2019b) AA-PHD (Li TC et al., 2017c, 2019a, 2019c, 2019d; Li TC and Hlawatsch, 2017; Gostar et al., 2017a) AA-CPHD (Yu et al., 2016; Da et al. 2020b; Gao et al., 2020b) AA-MeMber (Li TC et al., 2020b) AA-GLMB/LMB (Gao et al., 2019a) AA-PMBM (Li TC and Da, 2020)	GA-Bernoulli (Clark et al., 2010; Guldogan, 2014) GA-PHD (Clark et al., 2010; Üney et al., 2013) GA-CPHD (Clark et al., 2010; Battistelli et al., 2013) GA-MeMber (Wang et al. 2017) GA-GLMB/LMB (Jiang et al., 2016; Fantacci et al., 2018; Li SQ et al., 2017, 2019)

5.1.1 Fusion weight

According to the best fit of mixture principle (Li TC and Da, 2020), the optimal fusion weights $\boldsymbol{w}=[w_1,w_2,\ldots,w_n]^{\mathrm{T}}$ in GA/AA fusion need to be specified by minimizing a cost function:

$$\boldsymbol{w}=\underset{\sum_i w_i=1, w_i\in\boldsymbol{w}}{\arg\min}\ J(\boldsymbol{w}), \tag{39}$$

where the cost function $J(\boldsymbol{w})$ can be set as Fréchet functions in Eqs. (28)–(29), the sum of KLDs in Eqs. (30)–(31), or the Rényi divergence (Ristic et al., 2011).

In practice, however, it may turn out to be too complicated to solve Eq. (39) in real time. Instead, the fusion weights $\boldsymbol{w}$ are often specified directly through prior knowledge. For example, to ensure rapid convergence for consensus when the network is strongly connected, a popular choice is given by the so-called Metropolis weights (Xiao and Boyd, 2004). More advanced fusion-weight designs should take more network issues into account, such as dynamics and controllability (Papa et al., 2018; Xiang et al., 2019). Nevertheless, it was found that fixed and uniform fusion weights may lead to better performance, comparable to that of online optimization (Üney et al., 2011).

5.1.2 Communication mode

The majority of existing WSN-communication schemes can be classified in Fig. 5. Lying at the heart of these communication approaches is the distributed-consensus approach, which usually iterates for many rounds and communicates with all neighbors to achieve network convergence (Xiao and Boyd, 2004; Olfati-Saber et al., 2007). However, in this protocol the communication constraints and convergence needs in real-time filtering applications are not considered. To reduce the communication burden, three types of fusion strategies may be employed.

1. Under the Gossip algorithm (Boyd et al., 2006; Dias and Bruno, 2016; Yu et al., 2016), each sensor communicates only with some of its neighboring sensors at each iteration, for which the communication is reduced at the price of slower network convergence.

2. In an event-triggered strategy (Shi et al., 2014; Gao et al., 2019b), communication happens only when an event occurs, with the triggering conditions being a significant difference between the

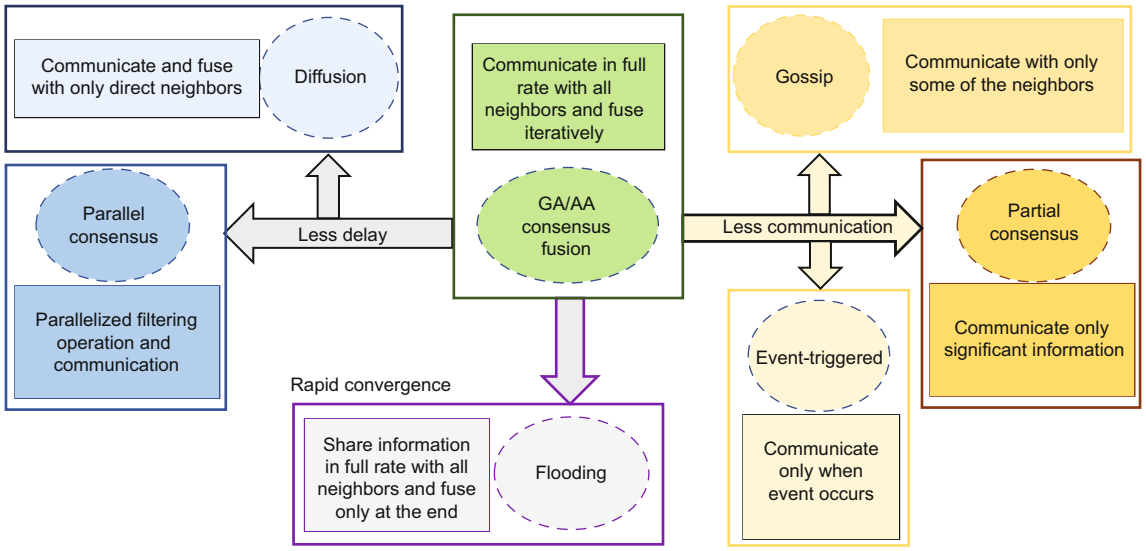

Fig. 5 Various network-communication modes of distinct strengths

current information and that of the latest broadcast or when the targets of interest are found.

3. The partial-consensus method (Li TC and Hlawatsch, 2017; Li TC et al., 2019d) transmits only significant information, rather than all information, between sensors in each iteration, while the insignificant residues are retained locally. The significant information (in terms of GCs typically) is distinguished based on its probabilities/weights, or its locations in the field of view.

To accelerate convergence, the distributed flooding scheme (Li TC et al., 2017b) can be applied in which each sensor collects the relevant information via iterative neighborhood communication and performs fusion only at the end of all communication iterations. This algorithm has the best deterministic convergence efficiency and will reach full convergence if the number of iterations is greater than the network's diameter. Furthermore, to reduce the communication delay, the following two network-communication modes can be considered:

1. The diffusion strategy (Sayed et al., 2018; Li TC et al., 2019c) only requires the sensor to communicate with its neighbor sensors once at each filtering iteration, no matter the convergence.

2. The parallel-filtering-communication mode (Li TC and Hlawatsch, 2017; Li TC et al., 2020a) aims to carry out filtering and communication/fusion in parallel, thereby preventing any delay caused to the filter due to communication; more details are given in the following subsection.

5.1.3 Parallel-filtering-communication mode

A majority of existing distributed-filtering algorithms rely on a serial filtering-communication mode (Fig. 6a). The internode communication is performed iteratively with filtering calculation. To avoid sensor-data delay, the sum of the numbers of calculation times for communication and for each filtering iteration must be smaller than that for the sensing iteration. This mode is, however, very restrictive in practice (Li TC and Hlawatsch, 2017; Li TC et al., 2020a). By contrast, the more practical and useful yet difficult mode is the parallel-filtering-communication mode (Fig. 6b) and was originally

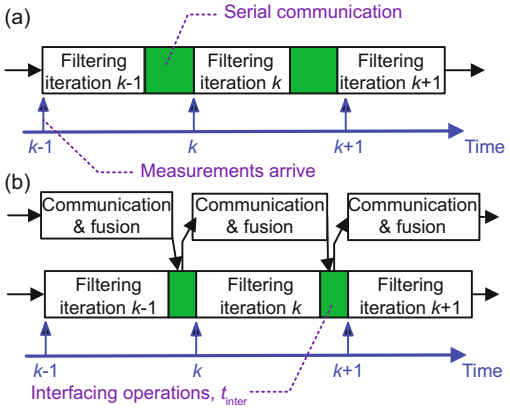

Fig. 6 Comparison between serial and parallel filtering-communication modes

References to color refer to the online version of this figure

demonstrated in Li TC and Hlawatsch (2017) and Li TC et al. (2020a). Here, communication can be performed in parallel with filtering operations and only a small amount of time (the green block) needs to be reserved for the interfacing operation.

Thanks to the importance-sampling approach, the particle implementation (Li TC and Hlawatsch, 2017) renders a higher level of parallel filtering-communication than the GM implementation (Li TC et al., 2020a). Further investigation is certainly significant in parallelizing the filtering and communication in the other distributed filter.

5.2 Dynamic or restrictive WSN

5.2.1 Sensor registration

A majority of existing multisensor tracking algorithms presume that the relative location of each sensor is known to others, which is the basis for relevant information fusion. This, however, is not satisfied when direct measurements of the sensors' location and orientation are unreliable. Thus, there must be more or less bias in matching the coordinates of different sensors (Fig. 7).

Assuming that the sensors are independent and that their measurements are conditionally independent, we have

$$f_k(\boldsymbol{b}, X|Z_k^{1:s}) \propto \prod_{i=1}^{s} g_k^i(Z_k^i|X, b^i) f_{k|k-1}(\boldsymbol{b}, X|Z_{k-1}^{1:s}), \tag{40}$$

where $\boldsymbol{b} = \left(b^1, b^2, \ldots, b^s\right)^{\mathrm{T}}$ is the joint-sensor-bias vector. Joint multisensor registration and MTT (JMRMTT) serves to estimate $\boldsymbol{b}$ and X simultaneously. A natural idea for this purpose is using the common information concerning the targets that the sensors observe. Representative examples are the Bayesian unified registration and tracking filter (Lian et al., 2011; Ristic et al., 2013a), distributed estimation based on pairwise Markov random-field models (Üney et al., 2015, 2018), and the Wasserstein-like distance between state estimates (Da et al., 2020a). The above approaches consider only translational biases, but ignore the rotational biases of the coordinate systems. Gao et al. (2020a) estimated the rotational biases by minimizing the KLD between the two posterior densities. However, first it suffers from complex high-dimensional calculation. Second, the KLD between densities not only is due to the difference in the coordinate systems but also is affected by many factors, such as false alarms and missed detections.

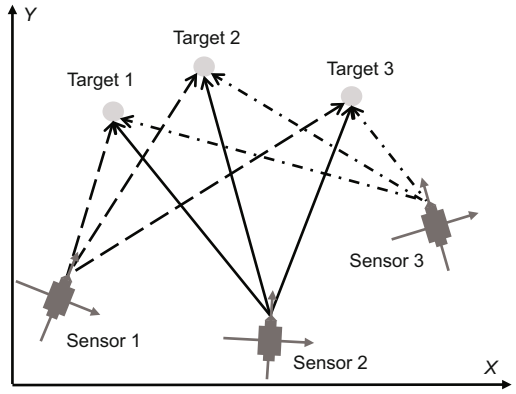

Fig. 7 Matching the coordinates of different sensors through their commonly observed targets

More dynamic network issues include time-varying typology and the addition/removal of nodes, which all affect the fusion-weight design and convergence of the fusion. There have also been fruitful works on sensor control. MTT and sensor control can be unified as a partially observed Markov-decision process, where the control command is usually given by solving an optimization problem (e.g., increasing the observability or reducing the error bound of the system) (Ristic et al., 2013a; Gostar et al., 2017b; Lian et al., 2018a, 2018b; Yan et al., 2020a, 2020b).

5.2.2 Limited fields of view

The fields of view (FoVs) of the sensors are usually limited and point in different directions (Liu et al., 2017), presenting a great challenge for multisensor fusion. One solution is to extend the prior FoVs of all sensors to an identical and larger FoV before fusion (Battistelli et al., 2017; Li SQ et al., 2018), but this may underestimate the existence probabilities of targets in non-public areas. Another widely used method is to split the information according to the FoVs' intersection (Gan et al., 2016; Vasic et al., 2016; Li TC et al., 2019c; Da et al., 2020b; Li GC et al., 2020). Fusion will be executed in each splitting area separately, followed by a reunion operation for all areas. Relevantly, a significant line of research is to constrain the directions and ranges of FoVs through sensor management (Mahler, 2007c; Chen YJ et al., 2017; Lian et al., 2018a, 2018b) to achieve balance between the surveillance range and the tracking performance.

5.3 More open issues

MTT fusion is clearly not a simple extension of single-target information fusion. Simply put, it does not make any sense to fuse between two different targets or between a target and a false alarm. Thus, data association is explicitly or implicitly needed in MTT fusion, for which achievements in traditional/non-RFS based (multisensor) MTT approaches might be useful. As one of the most focused information-fusion realms, multisensor RFS fusion deserves further research and still faces many challenges. To name a few:

1. Fusion beyond state: fusion of labels when the trajectories of targets are considered; fusion of extension properties when extended targets are considered; fusion between different types of MPDs including model information (Da et al., 2020b; He et al., 2020; Kim et al., 2020).

2. Fusion in parallel to the filtering calculation to accommodate different types of filters without networking delay—real-time performance is a need that will never be overemphasized in the context of tracking.

3. Fusion under abnormal/non-standard WSN conditions: sensor failure (Ramachandran et al., 2020), malicious nodes (Vempaty et al., 2013), time-varying topology and number of nodes, heterogeneous sensor configurations (Hu et al., 2020; Yan et al., 2020a), and so on.

Contributors

Kai DA and Tiancheng LI designed the research. Kai DA drafted the manuscript. Tiancheng LI revised the manuscript. Qiang FU and Yongfeng ZHU edited the manuscript and added references. Tiancheng LI and Hongqi FAN reviewed and finalized the paper.

Compliance with ethics guidelines

Kai DA, Tiancheng LI, Yongfeng ZHU, Hongqi FAN, and Qiang FU declare that they have no conflict of interest.

References

Abbas AE, 2009. A Kullback-Leibler view of linear and log-linear pools. *Dec Anal*, 6(1):25-37. https://doi.org/10.1287/deca.1080.0133

Bailey T, Julier S, Agamennoni G, 2012. On conservative fusion of information with unknown non-Gaussian dependence. Proc 15th Int Conf on Information Fusion, p.1876-1883.

Bar-Shalom Y, Willett PK, Tian X, 2011. Tracking and Data Fusion. YBS Publishing, USA.

Battistelli G, Chisci L, Fantacci C, et al., 2013. Consensus CPHD filter for distributed multitarget tracking. *IEEE J Sel Top Signal Process*, 7(3):508-520. https://doi.org/10.1109/JSTSP.2013.2250911

Battistelli G, Chisci L, Fantacci C, et al., 2014. Distributed peer-to-peer multitarget tracking with association-based track fusion. Proc 17th Int Conf on Information Fusion, p.1-7.

Battistelli G, Chisci L, Laurenzi A, 2017. Random set approach to distributed multivehicle SLAM. *IFAC*, 50(1):2457-2464. https://doi.org/10.1016/j.ifacol.2017.08.410

Beard M, Vo BT, Vo BN, et al., 2017. Void probabilities and Cauchy–Schwarz divergence for generalized labeled multi-Bernoulli models. *IEEE Trans Signal Process*, 65(19):5047-5061. https://doi.org/10.1109/TSP.2017.2723355

Blackman S, Blackman SS, Popoli R, 1999. Design and Analysis of Modern Tracking Systems. Artech House, Norwood, USA.

Boyd S, Ghosh A, Prabhakar B, et al., 2006. Randomized Gossip algorithms. *IEEE Trans Inform Theory*, 52(6):2508-2530. https://doi.org/10.1109/TIT.2006.874516

Buonviri A, York M, LeGrand K, et al., 2019. Survey of challenges in labeled random finite set distributed multisensor multi-object tracking. IEEE Aerospace Conf, p.1-12. https://doi.org/10.1109/AERO.2019.8742216

Chen X, Tharmarasa R, Kirubarajan T, 2014. Multitarget multisensor tracking. In: Theodoridis S, Chellappa R (Eds.), Academic Press Library in Signal Processing. Academic Press, USA, p.759-812. https://doi.org/10.1016/B978-0-12-396500-4.00015-6

Chen YJ, Zhang Q, Luo Y, et al., 2017. Multi-target radar imaging based on phased-MIMO technique—Part II: adaptive resource allocation. *IEEE Sens J*, 17(19):6198-6209. https://doi.org/10.1109/JSEN.2017.2740038

Chong CY, Mori S, Chang K, 1990. Distributed multitarget multisensory tracking. In: Bar-Shalom Y (Ed.), Multitarget-Multisensor Tracking: Advanced Applications. Artech House, Norwood, USA, p.247-295.

Chong CY, Chang KC, Mori S, 2018. A review of forty years of distributed estimation. Proc 21st Int Conf on Information Fusion, p.1-8. https://doi.org/10.23919/ICIF.2018.8455318

Clark D, Julier S, Mahler R, et al., 2010. Robust multi-object sensor fusion with unknown correlations. Proc Sensor Signal Processing for Defence, p.1-5. https://doi.org/10.1049/ic.2010.0233

Da K, Li TC, Zhu YF, et al., 2019. Kullback-Leibler averaging for multitarget density fusion. Proc Distributed Computing and Artificial Intelligence, p.253-261. https://doi.org/10.1007/978-3-030-23887-2_29

Da K, Li T, Zhu Y, et al., 2020a. A computationally efficient approach for distributed sensor localization and multitarget tracking. *IEEE Commun Lett*, 24(2):335-338. https://doi.org/10.1109/LCOMM.2019.2954888

Da K, Li T, Zhu YF, et al., 2020b. Gaussian mixture particle jump-Markov-CPHD fusion for multitarget tracking using sensors with limited views. *IEEE Trans Signal Inform Process Netw*, 6:605-616. https://doi.org/10.1109/TSIPN.2020.3016478

Delande E, Duflos E, Heurguier D, et al., 2010. Multi-target PHD Filtering: Proposition of Extensions to the Multi-Sensor Case. Research Report No. RR-7337, INRIA, French.

Delande E, Duflos E, Vanheeghe P, et al., 2011. Multi-sensor PHD: construction and implementation by space partitioning. Proc IEEE Int Conf on Acoustics, Speech and Signal Processing, p.3632-3635. https://doi.org/10.1109/ICASSP.2011.5947137

Dias SS, Bruno MGS, 2016. Distributed Bernoulli filters for joint detection and tracking in sensor networks. *IEEE Trans Signal Inform Process Netw*, 2(3):260-275. https://doi.org/10.1109/TSIPN.2016.2580460

Fantacci C, Papi F, 2016. Scalable multisensor multitarget tracking using the marginalized δ-GLMB density. *IEEE Signal Process Lett*, 23(6):863-867. https://doi.org/10.1109/LSP.2016.2557078

Fantacci C, Vo BT, Papi F, et al., 2015. The marginalized δ-GLMB filter. https://arxiv.org/abs/1501.00926

Fantacci C, Vo BN, Vo BT, et al., 2018. Robust fusion for multisensor multiobject tracking. *IEEE Signal Process Lett*, 25(5):640-644. https://doi.org/10.1109/LSP.2018.2811750

Farina A, Battistelli G, Chisci L, et al., 2017. 40 years of tracking for radar systems: a cross-disciplinary academic and industrial viewpoint. Int Conf on Control, Automation and Information Sciences, p.1-8. https://doi.org/10.1109/iccais.2017.8217557

Gan J, Vasic M, Martinoli A, 2016. Cooperative multiple dynamic object tracking on moving vehicles based on sequential Monte Carlo probability hypothesis density filter. Proc IEEE 19$^{\text{th}}$ Int Conf on Intelligent Transportation Systems, p.2163-2170. https://doi.org/10.1109/itsc.2016.7795906

Gao L, Battistelli G, Chisci L, 2019a. Fusion of labeled RFS densities with minimum information loss. https://arxiv.org/abs/1911.01083

Gao L, Battistelli G, Chisci L, 2019b. Event-triggered distributed multitarget tracking. *IEEE Trans Signal Inform Process Netw*, 5(3):570-584. https://doi.org/10.1109/TSIPN.2019.2924196

Gao L, Battistelli G, Chisci L, et al., 2020a. Distributed joint sensor registration and multitarget tracking via sensor network. *IEEE Trans Aerosp Electron Syst*, 56(2):1301-1317. https://doi.org/10.1109/TAES.2019.2929972

Gao L, Battistelli G, Chisci L, 2020b. Multiobject fusion with minimum information loss. *IEEE Signal Process Lett*, 27:201-205. https://doi.org/10.1109/LSP.2019.2963817

García-Fernández ÁF, Williams JL, Granström K, et al., 2018. Poisson multi-Bernoulli mixture filter: direct derivation and implementation. *IEEE Trans Aerosp Electron Syst*, 54(4):1883-1901. https://doi.org/10.1109/TAES.2018.2805153

Gostar AK, Hoseinnezhad R, Bab-Hadiashar A, 2017a. Cauchy-Schwarz divergence-based distributed fusion with Poisson random finite sets. Proc Int Conf on Control, Automation and Information Sciences, p.112-116. https://doi.org/10.1109/iccais.2017.8217559

Gostar AK, Hoseinnezhad R, Bab-Hadiashar A, et al., 2017b. Sensor-management for multitarget filters via minimization of posterior dispersion. *IEEE Trans Aerosp Electron Syst*, 53(6):2877-2884. https://doi.org/10.1109/TAES.2017.2718280

Gowing R, 2002. Roger Cotes Natural Philosopher. Cambridge University Press, Cambridge, UK.

Granström K, Lundquist C, Orguner U, 2010. A Gaussian mixture PHD filter for extended target tracking. Proc 13$^{\text{th}}$ Int Conf on Information Fusion, p.1-8. https://doi.org/10.1109/ICIF.2010.5711885

Granström K, Willett P, Bar-Shalom Y, 2015. Approximate multi-hypothesis multi-Bernoulli multi-object filtering made multi-easy. *IEEE Trans Signal Process*, 64(7):1784-1797. https://doi.org/10.1109/TSP.2015.2500884

Guldogan MB, 2014. Consensus Bernoulli filter for distributed detection and tracking using multi-static Doppler shifts. *IEEE Trans Aerosp Electron Syst*, 52(6):2732-2746. https://doi.org/10.1109/TAES.2016.150403

Gunay M, Orguner U, Demirekler M, 2016. Chernoff fusion of Gaussian mixtures based on sigma-point approximation. *IEEE Trans Aerosp Electron Syst*, 52(6):2732-2746. https://doi.org/10.1109/TAES.2016.150403

He S, Shin HS, Xu SY, et al., 2020. Distributed estimation over a low-cost sensor network: a review of state-of-the-art. *Inform Fus*, 54:21-43. https://doi.org/10.1016/j.inffus.2019.06.026

Heskes T, 1998. Selecting weighting factors in logarithmic opinion pools. Proc Conf on Advances in Neural Information Processing Systems, p.266-272.

Hlinka O, Slučiak O, Hlawatsch F, et al., 2012. Likelihood consensus and its application to distributed particle filtering. *IEEE Trans Signal Process*, 60(8):4334-4349. https://doi.org/10.1109/TSP.2012.2196697

Hu JW, Zheng BY, Wang C, et al., 2020. A survey on multi-sensor fusion based obstacle detection for intelligent ground vehicles in off-road environments. *Front Inform Technol Electron Eng*, 21(5):675-692. https://doi.org/10.1631/FITEE.1900518

Hurley MB, 2002. An information theoretic justification for covariance intersection and its generalization. Proc 5$^{\text{th}}$ Int Conf on Information Fusion, p.505-511. https://doi.org/10.1109/ICIF.2002.1021196

Javadi SH, Farina A, 2020. Radar networks: a review of features and challenges. *Inform Fus*, 61:48-55. https://doi.org/10.1016/j.inffus.2020.03.005

Jiang M, Yi W, Hoseinnezhad R, et al., 2016. Distributed multi-sensor fusion using generalized multi-Bernoulli densities. Proc 19$^{\text{th}}$ Int Conf on Information Fusion, p.1332-1339.

Julier SJ, 2006. An empirical study into the use of Chernoff information for robust, distributed fusion of Gaussian mixture models. 9$^{\text{th}}$ Int Conf on Information Fusion, p.1-8. https://doi.org/10.1109/ICIF.2006.301755

Julier SJ, 2008. Fusion without independence. Proc IET Seminar on Target Tracking and Data Fusion: Algorithms and Applications, p.1-4. https://doi.org/10.1049/ic:20080050

Julier SJ, Bailey T, Uhlmann JK, 2006. Using exponential mixture models for suboptimal distributed data fusion. IEEE Nonlinear Statistical Signal Processing Workshop, p.160-163. https://doi.org/10.1109/NSSPW.2006.4378844

Kim H, Granström K, Gao L, et al., 2020. 5G mmwave cooperative positioning and mapping using multi-model PHD filter and map fusion. *IEEE Trans Wirel Commun*, 19(6):3782-3795. https://doi.org/10.1109/TWC.2020.2978479

Li D, Wong KD, Hu YH, et al., 2002. Detection, classification, and tracking of targets. *IEEE Signal Process Mag*, 19(2):17-29. https://doi.org/10.1109/79.985674

Li GC, Battistelli G, Yi W, et al., 2020. Distributed multisensor multi-view fusion based on generalized covariance intersection. *Signal Process*, 166:107246. https://doi.org/10.1016/j.sigpro.2019.107246

Li SQ, Yi W, Hoseinnezhad R, et al., 2017. Robust distributed fusion with labeled random finite sets. *IEEE Trans Signal Process*, 66(2):278-293. https://doi.org/10.1109/TSP.2017.2760286

Li SQ, Battistelli G, Chisci L, et al., 2018. Multi-sensor multi-object tracking with different fields-of-view using the LMB filter. Proc 21st Int Conf on Information Fusion, p.1201-1208. https://doi.org/10.23919/ICIF.2018.8455250

Li SQ, Battistelli G, Chisci L, et al., 2019. Computationally efficient multi-agent multi-object tracking with labeled random finite sets. *IEEE Trans Signal Process*, 67(1):260-275. https://doi.org/10.1109/TSP.2018.2880704

Li TC, Da K, 2020. Best fit of mixture for distributed Poisson multi-Bernoulli mixture filtering. https://doi.org/10.36227/techrxiv.12351710

Li TC, Hlawatsch F, 2017. A distributed particle-PHD filter with arithmetic-average PHD fusion. http://arxiv.org/abs/1712.06128

Li TC, Corchado JM, Sun SD, et al., 2017a. Clustering for filtering: multi-object detection and estimation using multiple/massive sensors. *Inform Sci*, 388-389:172-190. https://doi.org/10.1016/j.ins.2017.01.028

Li TC, Corchado JM, Prieto J, 2017b. Convergence of distributed flooding and its application for distributed Bayesian filtering. *IEEE Trans Signal Inform Process Netw*, 3(3):580-591. https://doi.org/10.1109/TSIPN.2016.2631944

Li TC, Corchado JM, Sun SD, 2017c. On generalized covariance intersection for distributed PHD filtering and a simple but better alternative. Proc 20th Int Conf on Information Fusion, p.1-8. https://doi.org/10.23919/ICIF.2017.8009732

Li TC, Prieto J, Fan HQ, et al., 2018a. A robust multisensor PHD filter based on multi-sensor measurement clustering. *IEEE Commun Lett*, 22(10):2064-2067. https://doi.org/10.1109/LCOMM.2018.2863387

Li TC, Corchado JM, Chen HM, 2018b. Distributed flooding-then-clustering: a lazy networking approach for distributed multiple target tracking. Proc 21st Int Conf on Information Fusion, p.2415-2422. https://doi.org/10.23919/icif.2018.8455759

Li TC, Hlawatsch F, Djurić PM, 2019a. Cardinality-consensus-based PHD filtering for distributed multitarget tracking. *IEEE Signal Process Lett*, 26(1):49-53. https://doi.org/10.1109/LSP.2018.2878064

Li TC, Liu ZG, Pan Q, 2019b. Distributed Bernoulli filtering for target detection and tracking based on arithmetic average fusion. *IEEE Signal Process Lett*, 26(12):1812-1816. https://doi.org/10.1109/LSP.2019.2950588

Li TC, Elvira V, Fan HQ, et al., 2019c. Local-diffusion-based distributed SMC-PHD filtering using sensors with limited sensing range. *IEEE Sens J*, 19(4):1580-1589. https://doi.org/10.1109/jsen.2018.2882084

Li TC, Corchado JM, Sun SD, 2019d. Partial consensus and conservative fusion of Gaussian mixtures for distributed PHD fusion. *IEEE Trans Aerosp Electron Syst*, 55(5):2150-2163. https://doi.org/10.1109/TAES.2018.2882960

Li TC, Fan HQ, García J, et al., 2019e. Second-order statistics analysis and comparison between arithmetic and geometric average fusion: application to multi-sensor target tracking. *Inform Fus*, 51:233-243. https://doi.org/10.1016/j.inffus.2019.02.009

Li TC, Mallick M, Pan Q, 2020a. A parallel filtering-communication based cardinality consensus approach for real-time distributed PHD filtering. *IEEE Sens J*, in press. https://doi.org/10.1109/JSEN.2020.3004068

Li TC, Wang XX, Liang Y, et al., 2020b. On arithmetic average fusion and its application for distributed multi-Bernoulli multitarget tracking. *IEEE Trans Signal Process*, 68:2883-2896. https://doi.org/10.1109/TSP.2020.2985643

Lian F, Han C, Liu W, et al., 2011. Joint spatial registration and multi-target tracking using an extended probability hypothesis density filter. *IET Radar Sonar Navig*, 5(4):441-448. https://doi.org/10.1049/iet-rsn.2010.0057

Lian F, Hou LM, Liu J, et al., 2018a. Constrained multi-sensor control using a multi-target MSE bound and a δ-GLMB filter. *Sensors*, 18(7):2308. https://doi.org/10.3390/s18072308

Lian F, Hou LM, Wei B, et al., 2018b. Sensor selection for decentralized large-scale multi-target tracking network. *Sensors*, 18(12):4115. https://doi.org/10.3390/s18124115

Liggins ME, Hall DL, Llinas J, 2008. Handbook of Multisensor Data Fusion: Theory and Practice. CRC Press, Boca Raton, USA.

Liu WF, Chen YM, Cui HL, et al., 2017. Multi-sensor tracking with non-overlapping field for the GLMB filter. Proc Int Conf on Control, Automation and Information Sciences, p.197-202. https://doi.org/10.1109/ICCAIS.2017.8217575

Mahler R, 2000. Optimal/robust distributed data fusion: a unified approach. Proc Signal Processing, Sensor Fusion, and Target Recognition IX, p.128-138. https://doi.org/10.1117/12.395064

Mahler R, 2003. Multitarget Bayes filtering via first-order multitarget moments. *IEEE Trans Aerosp Electron Syst*, 39(4):1152-1178. https://doi.org/10.1109/TAES.2003.1261119

Mahler R, 2007a. PHD filters of higher order in target number. *IEEE Trans Aerosp Electron Syst*, 43(4):1523-1543. https://doi.org/10.1109/TAES.2007.4441756

Mahler R, 2007b. Statistical Multisource-Multitarget Information Fusion. Artech House, Norwood, USA.

Mahler R, 2007c. Unified sensor management using CPHD filters. Proc 10th Int Conf on Information Fusion, p.1-7. https://doi.org/10.1109/ICIF.2007.4407996

Mahler R, 2009a. The multisensor PHD filter: I. General solution via multitarget calculus. Proc Signal Processing, Sensor Fusion, and Target Recognition XVIII, Article 73360E. https://doi.org/10.1117/12.818024

Mahler R, 2009b. The multisensor PHD filter: II. Erroneous solution via "Poisson magic". Proc Signal Processing, Sensor Fusion, and Target Recognition XVIII, Article 73360D. https://doi.org/10.1117/12.818025

Mahler R, 2009c. PHD filters for nonstandard targets, I: extended targets. Proc 12th Int Conf on Information Fusion, p.915-921.

Mahler R, 2010. Approximate multisensor CPHD and PHD filters. Proc 13th Int Conf on Information Fusion, p.1-8. https://doi.org/10.1109/ICIF.2010.5711984

Mahler R, 2012. Toward a theoretical foundation for distributed fusion. In: Hall D, Chong CY, Llinas J, et al. (Eds.), Distributed Data Fusion for Network-Centric Operations. CRC Press, Boca Raton, FL, USA, p.199-224. https://doi.org/10.1201/b10124-8

Mahler R, 2013. "Statistics 102" for multisource-multitarget detection and tracking. *IEEE J Sel Top Signal Process*, 7(3):376-389. https://doi.org/10.1109/JSTSP.2013.2253084

Mahler R, 2014. Advances in Statistical Multisource-Multitarget Information Fusion. Artech House, Norwood, USA.

Meyer F, Kropfreiter T, Williams JL, et al., 2018. Message passing algorithms for scalable multitarget tracking. *Proc IEEE*, 106(2):221-259. https://doi.org/10.1109/jproc.2018.2789427

Musicki D, Evans R, 2004. Joint integrated probabilistic data association: JIPDA. *IEEE Trans Aerosp Electron Syst*, 40(3):1093-1099. https://doi.org/10.1109/TAES.2004.1337482

Nagappa S, Clark DE, 2011. On the ordering of the sensors in the iterated-corrector probability hypothesis density (PHD) filter. Proc Signal Processing, Sensor Fusion, and Target Recognition XX, Article 80500M. https://doi.org/10.1117/12.884618

Nannuru S, Blouin S, Coates M, et al., 2016. Multisensor CPHD filter. *IEEE Trans Aerosp Electron Syst*, 52(4):1834-1854. https://doi.org/10.1109/TAES.2016.150265

Nielsen F, Bhatia R, 2013. Matrix Information Geometry. Springer, Berlin, Germany. https://doi.org/10.1007/978-3-642-30232-9

Olfati-Saber R, Fax JA, Murray RM, 2007. Consensus and cooperation in networked multi-agent systems. *Proc IEEE*, 95(1):215-233. https://doi.org/10.1109/JPROC.2006.887293

Orguner U, Lundquist C, Granström K, 2011. Extended target tracking with a cardinalized probability hypothesis density filter. Proc 14th Int Conf on Information Fusion, p.1-8.

Ouyang C, Ji H, 2011. Scale unbalance problem in product multisensor PHD filter. *Electron Lett*, 47(22):1247-1249. https://doi.org/10.1049/el.2011.1843

Papa G, Repp R, Meyer F, et al., 2018. Distributed Bernoulli filtering using likelihood consensus. *IEEE Trans Signal Inform Process Netw*, 5(2):218-233. https://doi.org/10.1109/TSIPN.2018.2881718

Pham NT, Huang WM, Ong SH, 2007. Multiple sensor multiple object tracking with GMPHD filter. Proc 10th Int Conf on Information Fusion, p.1-7. https://doi.org/10.1109/ICIF.2007.4408087

Ramachandran RK, Fronda N, Sukhatme GS, 2020. Resilience in multi-robot multi-target tracking with unknown number of targets through reconfiguration. https://arxiv.org/abs/2004.07197

Reuter S, Vo BT, Vo BN, et al., 2014. The labeled multi-Bernoulli filter. *IEEE Trans Signal Process*, 62(12):3246-3260. https://doi.org/10.1109/TSP.2014.2323064

Ristic B, Vo BN, Clark D, 2011. A note on the reward function for PHD filters with sensor control. *IEEE Trans Aerosp Electron Syst*, 47(2):1521-1529. https://doi.org/10.1109/TAES.2011.5751278

Ristic B, Clark DE, Gordon N, 2013a. Calibration of multi-target tracking algorithms using non-cooperative targets. *IEEE J Sel Top Signal Process*, 7(3):390-398. https://doi.org/10.1109/JSTSP.2013.2256877

Ristic B, Vo BT, Vo BN, et al., 2013b. A tutorial on Bernoulli filters: theory, implementation and applications. *IEEE Trans Signal Process*, 61(13):3406-3430. https://doi.org/10.1109/TSP.2013.2257765

Saucan AA, Coates MJ, Rabbat M, 2017. A multisensor multi-Bernoulli filter. *IEEE Trans Signal Process*, 65(20):5495-5509. https://doi.org/10.1109/TSP.2017.2723348

Sayed AH, Djurić PM, Hlawatsch F, 2018. Distributed Kalman and particle filtering. In: Djurić PM, Richard C (Eds.), Cooperative and Graph Signal Processing. Academic Press, Amsterdam, USA, p.169-207. https://doi.org/10.1016/B978-0-12-813677-5.00006-7

Shi DW, Chen TW, Shi L, 2014. An event-triggered approach to state estimation with multiple point- and set-valued measurements. *Automatica*, 50(6):1641-1648. https://doi.org/10.1016/j.automatica.2014.04.004

Si WJ, Zhu HF, Qu ZY, 2020. Multi-sensor Poisson multi-Bernoulli filter based on partitioned measurements. *IET Radar Sonar Nav*, 14(6):860-869. https://doi.org/10.1049/iet-rsn.2019.0510

Smith J, Particke F, Hiller M, et al., 2019. Systematic analysis of the PMBM, PHD, JPDA, and GNN multi-target tracking filters. Proc 22th Int Conf on Information Fusion, p.1-8.

Streit R, Degen C, Koch W, 2015. The pointillist family of multitarget tracking filters. https://arxiv.org/abs/1505.08000

Sudderth EB, Ihler AT, Isard M, et al., 2010. Nonparametric belief propagation. *Commun ACM*, 53(10):95-103. https://doi.org/10.1145/1831407.1831431

Tsybakov AB, 2008. Introduction to Nonparametric Estimation. Springer Science & Business Media, New York, USA. https://doi.org/10.1007/b13794

Uhlmann JK, 1996. General data fusion for estimates with unknown cross covariances. Proc Signal Processing, Sensor Fusion, and Target Recognition V, p.536-548. https://doi.org/10.1117/12.243195

Üney M, Julier S, Clark D, et al., 2010. Monte Carlo realisation of a distributed multi-object fusion algorithm. Proc Sensor Signal Processing for Defence, p.1-5. https://doi.org/10.1049/ic.2010.0232

Üney M, Clark DE, Julier SJ, 2011. Information measures in distributed multitarget tracking. Proc 14th Int Conf on Information Fusion, p.1-8.

Üney M, Clark DE, Julier SJ, 2013. Distributed fusion of PHD filters via exponential mixture densities. *IEEE J Sel Top Signal Process*, 7(3):521-531. https://doi.org/10.1109/JSTSP.2013.2257162

Üney M, Mulgrew B, Clark DE, 2015. A cooperative approach to sensor localisation in distributed fusion networks. *IEEE Trans Signal Process*, 64(5):1187-1199. https://doi.org/10.1109/TSP.2015.2493981

Üney M, Mulgrew B, Clark DE, 2018. Latent parameter estimation in fusion networks using separable likelihoods. *IEEE Trans Signal Inform Process Netw*, 4(4):752-768. https://doi.org/10.1109/TSIPN.2018.2825599

Üney M, Houssineau J, Delande E, et al., 2019. Fusion of finite-set distributions: pointwise consistency and global cardinality. *IEEE Trans Aerosp Electron Syst*, 55(6):2759-2773. https://doi.org/10.1109/TAES.2019.2893083

Vasic M, Mansolino D, Martinoli A, 2016. A system implementation and evaluation of a cooperative fusion and tracking algorithm based on a Gaussian mixture PHD filter. Proc IEEE/RSJ Int Conf on Intelligent Robots and Systems, p.4172-4179. https://doi.org/10.1109/IROS.2016.7759614

Vempaty A, Tong L, Varshney PK, 2013. Distributed inference with Byzantine data: state-of-the-art review on data falsification attacks. *IEEE Signal Process Mag*, 30 (5):65-75. https://doi.org/10.1109/MSP.2013.2262116

Vo BN, Ma WK, 2006. The Gaussian mixture probability hypothesis density filter. *IEEE Trans Signal Process*, 54(11):4091. https://doi.org/10.1109/TSP.2006.881190

Vo BN, Vo BT, 2019. A multi-scan labeled random finite set model for multi-object state estimation. *IEEE Trans Signal Process*, 67(19):4948-4963. https://doi.org/10.1109/TSP.2019.2928953

Vo BN, Singh S, Doucet A, 2005. Sequential Monte Carlo methods for multitarget filtering with random finite sets. *IEEE Trans Aerosp Electron Syst*, 41(4):1224-1245. https://doi.org/10.1109/TAES.2005.1561884

Vo BN, Vo BT, Phung D, 2014. Labeled random finite sets and the Bayes multi-target tracking filter. *IEEE Trans Signal Process*, 62(24):6554-6567. https://doi.org/10.1109/TSP.2014.2364014

Vo BN, Mallick M, Bar-Shalom Y, et al., 2015. Multitarget tracking. In: Webster JG (Ed.), Wiley Encyclopedia of Electrical and Electronics Engineering. John Wiley & Sons, Inc., NJ, USA, p.1-15. https://doi.org/10.1002/047134608X.W8275

Vo BN, Vo BT, Beard M, 2019. Multi-sensor multi-object tracking with the generalized labeled multi-Bernoulli filter. *IEEE Trans Signal Process*, 67(23):5952-5967. https://doi.org/10.1109/TSP.2019.2946023

Vo BT, 2008. Random Finite Sets in Multi-object Filtering. PhD Thesis, University of Western Australia, Australia.

Vo BT, Vo BN, 2013. Labeled random finite sets and multi-object conjugate priors. *IEEE Trans Signal Process*, 61(13):3460-3475. https://doi.org/10.1109/TSP.2013.2259822

Vo BT, Vo BN, Cantoni A, 2007. Analytic implementations of the cardinalized probability hypothesis density filter. *IEEE Trans Signal Process*, 55(7):3553-3567. https://doi.org/10.1109/TSP.2007.894241

Vo BT, Vo BN, Cantoni A, 2009. The cardinality balanced multi-target multi-Bernoulli filter and its implementations. *IEEE Trans Signal Process*, 57(2):409-423. https://doi.org/10.1109/TSP.2008.2007924

Vo BT, Vo BN, Hoseinnezhad R, et al., 2013. Robust multi-Bernoulli filtering. *IEEE J Sel Top Signal Process*, 7(3):399-409. https://doi.org/10.1109/JSTSP.2013.2252325

Wang BL, Yi W, Li S, et al., 2015. Distributed multi-target tracking via generalized multi-Bernoulli random finite sets. Proc 18th Int Conf on Information Fusion, p.253-261.

Wang BL, Yi W, Hoseinnezhad R, et al., 2017. Distributed fusion with multi-Bernoulli filter based on generalized covariance intersection. *IEEE Trans Signal Process*, 65(1):242-255. https://doi.org/10.1109/TSP.2016.2617825

Wei BS, Nener B, Liu WF, et al., 2016. Centralized multi-sensor multi-target tracking with labeled random finite sets. Proc Int Conf on Control, Automation and Information Sciences, p.82-87. https://doi.org/10.1109/ICCAIS.2016.7822440

Willett P, Ruan Y, Streit R, 2002. PMHT: problems and some solutions. *IEEE Trans Aerosp Electron Syst*, 38(3):738-754. https://doi.org/10.1109/TAES.2002.1039396

Williams JL, 2015. Marginal multi-Bernoulli filters: RFS derivation of MHT, JIPDA, and association-based MeMBer. *IEEE Trans Aerosp Electron Syst*, 51(3):1664-1687. https://doi.org/10.1109/TAES.2015.130550

Xia YX, Granstrcom K, Svensson L, et al., 2017. Performance evaluation of multi-Bernoulli conjugate priors for multi-target filtering. Proc 20th Int Conf on Information Fusion, p.1-8. https://doi.org/10.23919/ICIF.2017.8009710

Xiang LY, Chen F, Ren W, et al., 2019. Advances in network controllability. *IEEE Circ Syst Mag*, 19(2):8-32. https://doi.org/10.1109/MCAS.2019.2909446

Xiao L, Boyd S, 2004. Fast linear iterations for distributed averaging. *Syst Contr Lett*, 53(1):65-78. https://doi.org/10.1016/j.sysconle.2004.02.022

Yan JK, Pu WQ, Zhou SH, et al., 2020a. Optimal resource allocation for asynchronous multiple targets tracking in heterogeneous radar network. *IEEE Trans Signal Process*, 68:4055-4068. https://doi.org/10.1109/TSP.2020.3007313

Yan JK, Pu WQ, Zhou SH, et al., 2020b. Collaborative detection and power allocation framework for target tracking in multiple radar system. *Inform Fus*, 55: 173-183. https://doi.org/10.1016/j.inffus.2019.08.010

Yu JY, Coates M, Rabbat M, 2016. Distributed multi-sensor CPHD filter using pairwise Gossiping. Proc IEEE Int Conf on Acoustics, Speech and Signal Processing, p.3176-3180. https://doi.org/10.1109/ICASSP.2016.7472263